VII International Conference on Computational Methods in Marine Engineering
MARINE 2017
M. Visonneau, P. Queutey and D. Le Touzé (Eds)

ACCELERATED FREE-SURFACE FLOW SIMULATIONS WITH INTERACTIVELY MOVING BODIES

ARTHUR E.P. VELDMAN*, HENK SEUBERS*, PETER VAN DER PLAS* AND JOOP HELDER†

* Institute for Mathematics and Computer Science, University of Groningen,
P.O. Box 407, 9700 AK Groningen, The Netherlands
e-mail: {a.e.p.veldman, h.seubers, p.van.der.plas}@rug.nl
web page: http://www.math.rug.nl/∼veldman/comflow/comflow.html

† MARIN, P.O. Box 28, 6700 AA Wageningen, The Netherlands
e-mail: j.helder@marin.nl

Key words: Computational Fluid Dynamics, fluid solid-body interaction, strong coupling, added mass, floating objects, free-fall life boat

Abstract. One of the challenges of simulating free-surface flow around moored or floating objects is the modelling, including the algorithmic coupling, of objects whose dynamics is determined by a two-way interaction with the incoming waves. The 'traditional' way of numerically coupling the flow dynamics with the dynamics of a floating object becomes unstable (or requires severe underrelaxation) when the added mass is larger than the mass of the object. To deal with this two-way interaction, a more simultaneous type of numerical coupling is being developed. The quasi-simultaneous method will be demonstrated on a number of simulation results for engineering applications from the offshore industry: the motion of a moored TLP platform in extreme waves, and the launch of a free-fall life boat.

1 INTRODUCTION

Simulating the hydrodynamics of floating structures using a two-way partitioned coupling poses a challenge when the coupling between the fluid and the structure is strong. The incompressibility of the fluid plays an important role, and leads to strong coupling when the ratio of so-called added mass to structural mass is considerate. Existing fluid-structure interaction procedures become less efficient in such cases, and can even become unstable [1, 2]. This paper proposes a coupling method that deals with the added-mass effect by anticipation, and remains stable and efficient at all times.

Physically, the interaction between incoming waves and a structure can be labelled as one-way or two-way. In the former case the structure 'simply' reacts to the oncoming flow

field, but in the latter case the motion of the structure influences the flow field around the structure. The latter case poses most challenges to the numerical coupling between flow and structure. A numerical coupling approach can be aggregated (monolithic) or segregated (partitioned). In the former case, all discrete equations are combined into one single set of equations. In the latter case, two separate discrete systems (modules) can be recognized equipped with recipes to exchange information. This enhances the flexibility of the approach, but it also requires an iterative exchange of information with its consequences for numerical stability [3, 4]. The paper describes our efforts to find a compromise between the robust monolithic approach and the more flexible but vulnerable partitioned approach

The structural model consists of a rigid body with elastic mooring lines, and the fluid is modelled by a volume-of-fluid method for the free surface [5]. Instead of imposing the structural displacement to the fluid, a combination of pressure and displacement is prescribed that approximates the body dynamics [6]. Through this modified boundary condition, the flow can anticipate the structural motion. This anticipatory, quasi-simultaneous coupling method increases the numerical efficiency, while the results are - by design - the same as in the usual formulation.

To demonstrate the new method, a number of simulation results for engineering applications from the offshore industry will be presented, such as the motion of a moored TLP platform in extreme waves, and the launch of a free-fall life boat.

Figure 1: Drop test with free-fall lifeboat (from: www.verhoef.eu)

2 MATHEMATICAL FLOW MODEL

Incompressible, turbulent fluid flow can be modelled by means of the Navier–Stokes equations.

$$\mathcal{D}\mathbf{u} = 0, \qquad \frac{\partial \mathbf{u}}{\partial t} + \mathcal{C}(\mathbf{u})\mathbf{u} + \mathcal{G}p - \mathcal{V}\mathbf{u} = \mathbf{f}. \tag{1}$$

Here $\mathcal{D}$ is the divergence operator describing conservation of mass. Conservation of momentum is based on the convection operator $\mathcal{C}(\mathbf{u})\mathbf{v} \equiv \nabla(\mathbf{u} \otimes \mathbf{v})$, the pressure gradient operator $\mathcal{G} = \nabla$, the viscous diffusion operator $\mathcal{V}(\mathbf{u}) \equiv \nabla \cdot \nu \nabla \mathbf{u}$ and a forcing term $\mathbf{f}$. The kinematic viscosity is denoted by ν.

Turbulence is modelled by means of large-eddy simulation (LES) using a low-dissipation QR-model as formulated by Verstappen [7]; for its use in maritime applications, see [8,9]. This model has been refined and extended in the PhD thesis of Rozema [10] towards the so-called anisotropic minimum dissipation (AMD) model, which can be applied at (highly) anisotropic computational grids. It is being further explored in cooperation with the Center for Turbulent Research (Stanford University) [11–13].

The Navier–Stokes equations (1) are discretized on an Arakawa C-grid. The second-order finite-volume discretization of the continuity equation at the 'new' time level $\cdot^{n+1}$ is given by

$$\mathcal{D}^0 \mathbf{u}^{n+1} = -\mathcal{D}^\Gamma \mathbf{u}_\Gamma^{n+1}, \tag{2}$$

where $\mathcal{D}^0$ acts on the interior of the domain and $\mathcal{D}^\Gamma$ acts on the boundaries of the domain (with $\mathbf{u}_\Gamma$ denoting the velocity at the boundary). In the discretized momentum equation, convection $\mathcal{C}(\mathbf{u}_h)$ and viscous diffusion $\mathcal{V}$ are discretized explicitly in time. The pressure gradient is discretized at the new time level. In this exposition, for readability reasons the first-order forward Euler time integration will be used. In the actual simulations, a second-order Adams–Bashforth method is being applied.

Letting the diagonal matrix Ω denote the matrix containing the geometric size of the control volumes, gives the discretized momentum equation as

$$\Omega \frac{\mathbf{u}^{n+1} - \mathbf{u}^n}{\delta t} = -\mathcal{C}(\mathbf{u}^n)\,\mathbf{u}^n + \mathcal{V}\mathbf{u}^n - \mathcal{G}p^{n+1} + \mathbf{f}. \tag{3}$$

For divergence-free velocity fields $\mathbf{u}$, the conservative discrete convection operator is skew-symmetric. In this way, the discrete convection does not contribute to energy production or dissipation; see Verstappen and Veldman [14]. In particular, its discretization preserves the energy of the flow and does not produce any artificial diffusion. To make the discretization fully energy-preserving, the discrete gradient operator and the divergence operator must be each other's negative transpose, i.e. $\mathcal{G} = -\mathcal{D}^{0T}$, thus mimicking the analytic symmetry $\nabla = -(\nabla\cdot)^T$. Then, also the work done by the pressure vanishes discretely. The latter is computed in the standard way from the Poisson equation obtained by combining (2) and (3).

The liquid region and the free liquid surface are described by an improved VOF-method; see e.g. Hirt and Nichols [15], Kleefsman et al. [5] and Düz [16].

3 FLUID–SOLID BODY COUPLING

A further step is to allow the moving object to interact with the fluid dynamics, e.g. it is floating on the water surface. This physical two-way coupling has to be mirrorred in

the numerical coupling algorithm between the flow solver and the solid-body solver. The coupling takes place along the common interface Γ between the fluid and the solid body; quantities involved are the dynamics (position and acceleration) of the solid body, and the dynamics of the fluid (in particular its pressure loads); see Fig. 2.

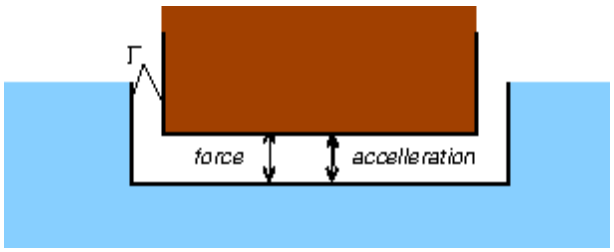

Figure 2: Schematic partitioning between fluid and solid body, with information exchange along their common interface Γ.

1. The *coupling conditions* at the interface between fluid and solid body basically express 'continuity' of the physics on both sides of the common interface Γ. The *kinematic* condition expresses that the boundary of the liquid region (partially) coincides with the surface of the solid body. In particular, material particles on both sides have the same velocity and acceleration (when the no-slip condition does not hold, only the normal velocity component is continuous). Hence, it makes sense to talk about the velocity at the interface $\mathbf{u}_\Gamma$. Additionally, the *dynamic* coupling condition is based on Newton's 3^{rd} law "$action = -reaction$", which expresses equilibrium of forces. In particular, we denote the fluid pressure by p_Γ. In the sequel, we will formulate the coupled problem in terms of the two interface variables: the velocity $\mathbf{u}_\Gamma$ and the integrated (force and moment) pressure load $\mathcal{F}(p_\Gamma)$ (short: $\mathcal{F}_\Gamma$).

2. The *solid-body dynamics* is governed by an equation describing the accelaration $\dot{\mathbf{u}}$ of the solid body when reacting to the forces and moments $\mathbf{f}$ excerted by the fluid. The latter are found by integration of the liquid pressure over the common interface Γ. In abstract terms we denote this relation by

$$\text{solid body dynamics:} \qquad M_{\text{sb}}\dot{\mathbf{u}}_\Gamma = \mathcal{F}_\Gamma. \tag{4}$$

   The mass operator M_{sb} (6 DOF) describes the intertial properties of the solid body, thus the eigenvalues of M_{sb} are porportional to the body mass and its moments of inertia. The load operator $\mathcal{F}_\Gamma$ involves the integration of the fluid pressure p_Γ over the interface to obtain the force and moments acting on the body. Note that we do not show eventual external forces, as they play no essential role in the coupling algorithm.

3. The *fluid dynamics* governs the reaction of the fluid to the motion of the solid body. The latter creates a boundary condition along the interface Γ which has to be added to the Navier–Stokes equations (1). As a result, the pressure loads along the interface and acting on the solid body can be computed. In abstract notation we write

$$\text{fluid dynamics:} \qquad \mathcal{F}_\Gamma = -M_{\text{ad}}\dot{\mathbf{u}}_\Gamma, \tag{5}$$

where M_{ad} is, by definition, the so-called *added mass* operator. Again, terms in $\mathbf{u}$ have been omitted because of their minor role in the analysis of the coupling process.

The above formulation (4)+(5) in principle shows two equations for the two unknowns along the interface: loads and acceleration. Their coupling can be done in an aggregated or segregated way. An aggregated (or strong) coupling recombines both equations (or modules) into one single global system which is solved simultaneously. In contrast, a segregated (or weak) coupling keeps the two equations apart and solves them in an iterative way. The former (monolithic) approach may not always be possible, e.g. due to their 'black-box' character, or due to the large complexity of the modules; the latter (partitioned) approach may diverge.

3.1 Weak coupling

In practice, often a segregated approach is followed. The usual way is to let the fluid determine the load field (= integrated pressure forces) $\mathcal{F}_\Gamma^{\text{old}}$ which moves the solid body:

$$M_{\text{sb}}\dot{\mathbf{u}}_\Gamma^{\text{new}} = \mathcal{F}_\Gamma^{\text{old}}. \tag{6}$$

This motion of the solid body is then transferred to the fluid, to react with a new pressure field:

$$\mathcal{F}_\Gamma^{\text{new}} = -M_{\text{ad}}\dot{\mathbf{u}}_\Gamma^{\text{new}}. \tag{7}$$

In this way, we effectively have created an iterative process

$$\mathcal{F}_\Gamma^{\text{new}} = -M_{\text{ad}}M_{\text{sb}}^{-1}\mathcal{F}_\Gamma^{\text{old}}. \tag{8}$$

The iterations in such a weak coupling method will converge if and only if the spectral radius of the iteration matrix $\rho(M_{\text{ad}}M_{\text{sb}}^{-1}) < 1$. Thus, this convergence condition is a requirement for the ratio between added mass and body mass. Roughly speaking, the solid body should be heavy enough. If it is not, underrelaxation can help achieving convergence, but this will require (many) additional (sub)iterations and diminishes efficiency.

In practice, such iterations can be implemented as follows in the solution process for the Navier–Stokes equation (3) during the time step from $n \to n+1$. An additional subiteration process (with iteration count k) is included:

$$\text{solid-body dynamics:} \qquad M_{\text{sb}}(\dot{\mathbf{u}}_\Gamma^{n+1})^k = (\mathcal{F}_\Gamma^{n+1})^k; \tag{9}$$

$$\text{Navier–Stokes:} \qquad (\mathcal{F}_\Gamma^{n+1})^{k+1} = -M_{\text{ad}}(\dot{\mathbf{u}}_\Gamma^{n+1})^k. \tag{10}$$

If necessary, these subiterations can be made convergent by applying (severe) underrelaxation without disturbing the time accuracy of the time integration method, but often at a considerable computational price.

Below we will demonstrate with an example of a falling life boat how many subiterations can be required in practical situations. Because of this inefficiency, it is better to apply an aggregated approach (which does not require subiterations), or at least to be as close as possible to such an approach. Such an approach is the quasi-simultaneous method, originally developed for interacting aerodynamic boundary layers along airplane wings [17]; a historic overview is provided in [18, 19].

3.2 Quasi-simultaneous coupling

For iterative efficiency reasons, it is worthwhile to follow the monolithic, simultaneous approach as much as possible. With the full dynamics operator $M_{\rm sb}$ being too complex, a good approximation is sought $\widetilde{M}_{\rm sb}$ which anticipates the reaction of the full dynamics $M_{\rm sb}$ and which is simple enough to be used as a boundary condition inside the Navier–Stokes solver (1). Such an approximation has been termed an *interaction law* [17–19]

$$\widetilde{M}_{\rm sb}\dot{\mathbf{u}}_\Gamma = \mathcal{F}_\Gamma. \tag{11}$$

The interaction law (11) is then incorporated in the time integration process in defect formulation:

$$\text{interaction law:} \qquad \dot{\mathbf{u}}_\Gamma^{n+1} - \widetilde{M}_{\rm sb}^{-1}\mathcal{F}_\Gamma^{n+1} = (M_{\rm sb}^{-1} - \widetilde{M}_{\rm sb}^{-1})\mathcal{F}_\Gamma^n \tag{12}$$

$$\text{Navier–Stokes:} \qquad \mathcal{F}_\Gamma^{n+1} + M_{\rm ad}\dot{\mathbf{u}}_\Gamma^{n+1} = 0. \tag{13}$$

Another interpretation in terms of time integration is that the part $\widetilde{M}_{\rm sb}$ of the dynamics equation (4) is treated implicitly and the remaining part $M_{\rm sb} - \widetilde{M}_{\rm sb}$ explicitly.

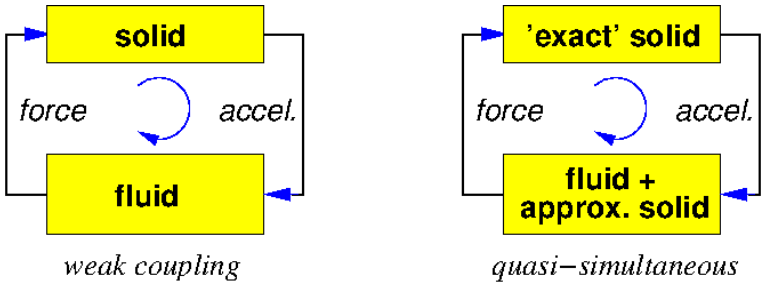

Figure 3: Weak versus quasi-simultaneous coupling.

The interaction law is a boundary condition for the Navier–Stokes equations along the interface Γ. More precisely, it will be implemented as a boundary condition for the

pressure Poisson equation.The latter is derived by first rewriting the boundary condition (12) for $\mathbf{u}$ as

$$\mathbf{u}_\Gamma^{n+1} - \delta t\, \widetilde{M}_{\rm sb}^{-1}\mathcal{F}(p_\Gamma^{n+1}) = \mathbf{u}_\Gamma^{n} + \delta t\, (M_{\rm sb}^{-1} - \widetilde{M}_{\rm sb}^{-1})\mathcal{F}(p_\Gamma^{n}).$$

Then the discrete momentum equation is written in the form (2), wherein the above relation is substituted through the term $\mathcal{D}^\Gamma\mathbf{u}_\Gamma$. Finally a relation is obtained featuring $\mathcal{F}_\Gamma$ as a boundary condition for the Poisson equation; see also [20].

The above *quasi-simultaneous* integration can be analysed by eliminating $\dot{\mathbf{u}}$ from (12)+(13), which leads to

$$(I + M_{\rm ad}\widetilde{M}_{\rm sb}^{-1})\mathcal{F}_\Gamma^{n+1} = -M_{\rm ad}(M_{\rm sb}^{-1} - \widetilde{M}_{\rm sb}^{-1})\mathcal{F}_\Gamma^{n}. \tag{14}$$

For $\widetilde{M}_{\rm sb}^{-1} \equiv 0$, the iteration process (8) is recovered, which breaks down when $M_{\rm ad}$ is 'too large'. But with the term $M_{\rm ad}\widetilde{M}_{\rm sb}^{-1}$ on the left-hand side and the difference $M_{\rm sb}^{-1} - \widetilde{M}_{\rm sb}^{-1}$ on the right-hand side, it will be clear that this process will converge when $\widetilde{M}_{\rm sb}$ is sufficiently close to $M_{\rm sb}$, in spite of a possibly 'large' $M_{\rm ad}$.

4 EXAMPLES

To show the performance of the quasi-simultaneous approach, two test cases are presented: i) a free-fall life boat; and ii) a moored TLP platform.

4.1 Falling life boat

The first test case is a simulation of a life boat dropped into calm water. Four snapshots of the simulation are shown in Fig. 4. The dynamics of the life boat is modelled by means of a 6-DOF mechanical model.

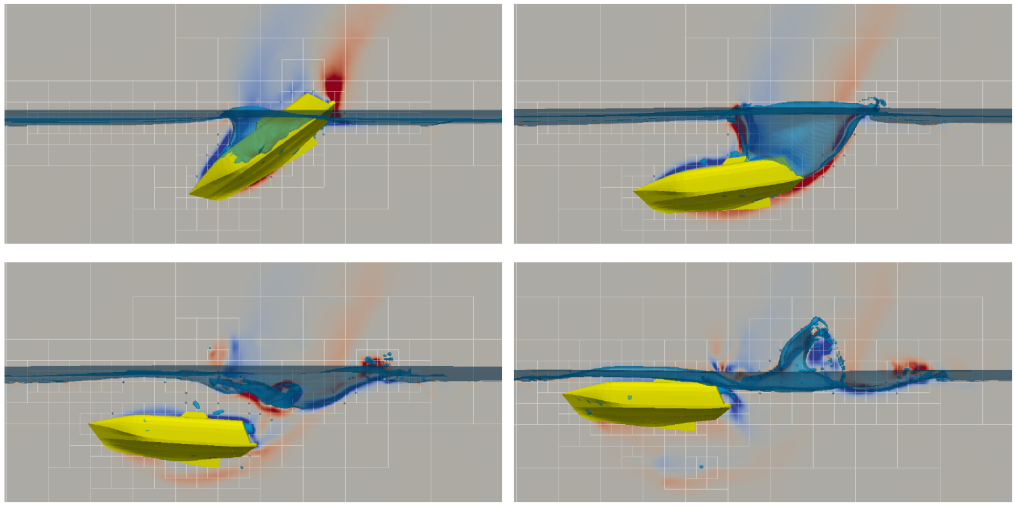

Figure 4: Four simulation snapshots of the drop of a life boat into calm water. The colors represent vorticity; the locally refined regions are indicated.

The fluid flow is modelled with the Navier-Stokes equations and solved on a grid consisting of about 0.5 million active (i.e. within the fluid) grid points, with local grid refinement [21, 22] around the life boat (Fig. 4).

For physical accuracy this grid is rather coarse, but the focus in these simulations is on the numerical behaviour of the coupling process. Thus both the weak coupling procedure (8) as well as the quasi-simultaneous procedure (13) have been applied. In the latter case, the interaction law is based on the under-water part of the lifeboat (as the Poisson equation is only solved under water).

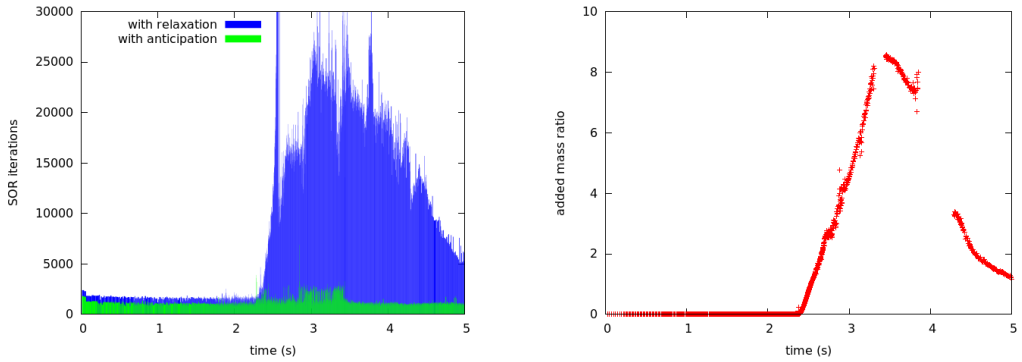

Figure 5: *Left:* The number of SOR iterations per time step for the underrelaxed weak coupling method (blue) and the anticipatory quasi-simultaneous method (green)). *Right:* The estimated added mass for the falling lifeboat as a function of time. The crossing of the free surface is clearly visible in the added mass.

The most important result concerns the amount of work that is needed per time step to achieve the coupling between solid-body dynamics and fluid flow. The weak method often requires dozens of subiterations, in each of which a Poisson equation has to be solved. This number is dependent on the amount of fluid that is moved aside by the moving body, represented by the added-mass operator M_a. To be fair, the later subiterations have a good initial guess so they are not as expensive as the earlier ones. Thus the amount of work is better represented by the total number of ierations, in this case SOR [23], that is needed for all Poisson solves within one time step. For other matrix solvers, the situation is relatively similar, as the number of required Poisson solves is basically independent of the solver choice.

The amount of work for a typical simulation (actually another one than presented in Fig. 4) is shown in Fig. 5(left). The close relation with the added mass becomes visible when plotting the time history of the estimated added mass in Fig. 5(right). Note that the 'gaps' in the curve are due to loss of figures during the estimation of the added mass. Comparison with Fig. 5(left) shows clearly that the number of iterations grows rapidly when the 'added-mass ratio' $\rho\left(M_{\mathrm{ad}}M_{\mathrm{sb}}^{-1}\right)$ growths beyond 1. In contrast, the quasi-simultaneous method requires only 1 or 2 subiterations (with additional Poisson solver), resulting in much less work per time step (Fig. 5(left)). This reduction in the

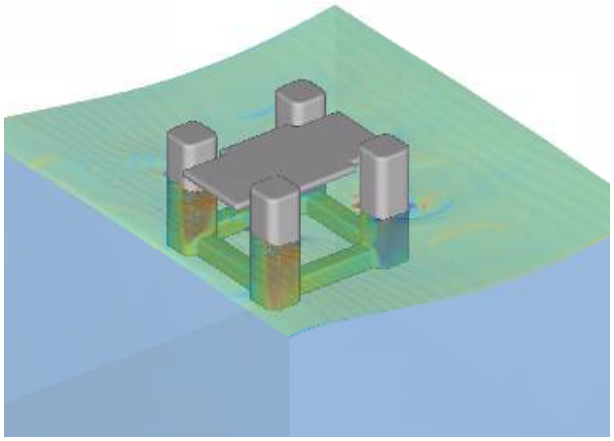

Figure 6: A snapshot from the simulation of a tension-leg platform in a Stokes-5 wave.

number of subiterations is highly independent of the grid size and of the chosen Poisson solver. More specifically, the number of subiterations is (to first order) only dependent on the difference between the analytic pendants of M_{sb} and $\widetilde{M}_{\mathrm{sb}}$.

The added mass varies greatly over time during the impact, as the boat enters the water and a larger part of the wave has to respond. It is clear that the relaxation-based method (9)+(10) is sensitive to this ratio, as the workload increases during the entry phase. The anticipative method (12)+(13) however remains efficient regardless of the added-mass ratio, as the boundary condition inside the wave simulation predicts the boat motion. It is observed that in this application the workload is reduced by a factor around 10 for the complete simulation.

4.2 Moored TLP

The second test case is a tension-leg platform in a long-crested wave. The platform is modelled as a rigid 6-DOF body with elastic mooring lines. It can perform large but finite translations and rotations in three dimensions, but it cannot deform or change in volume. The generalization of the algorithmic coupling method to deformable bodies is presented in a paper at this year's OMAE conference [6].

The incoming wave is a nonlinear 5th-order Stokes wave. Since the variations around the waterline are small compared to the size of the platform, the added-mass ratio is relatively constant. Even for this moderate added-mass ratio however, the anticipative method outperforms the relaxation-based method by a factor 2.5 to 3.

5 CONCLUSIONS

The ComFLOW simulation method has been designed to simulate and study extreme waves and their impact on falling, floating and moored structures. In particular, in this paper the interaction between the dynamics of a structure and the oncoming wave field

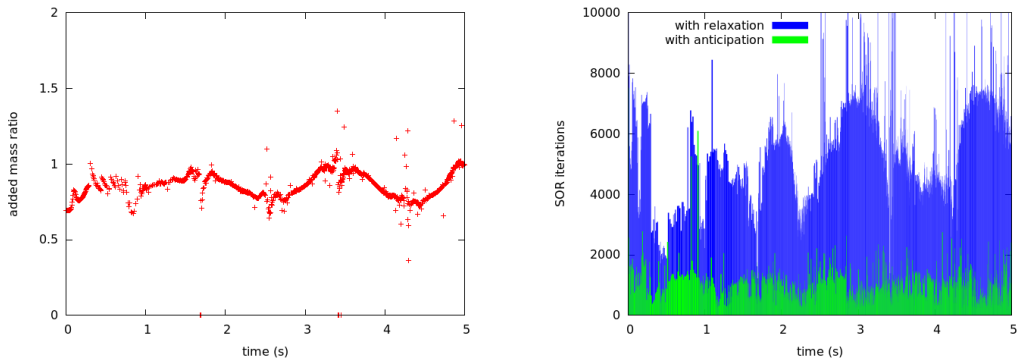

Figure 7: Workload of the simulation of a tension-leg platform in a Stokes-5 wave. *Left*: Variation of the effective added-mass ratio over time. *Right*: The workload for the simulation corresponds to the area under the curve.

is investigated. The efficiency of the numerical coupling algorithm is largely determined by the added-mass ratio, which seriously affects the existing partitioned coupling schemes based on the (sequential) exchange of loads and motions: a stronger coupling with a higher range of added-mass ratios leads to loss of performance in these traditional coupling schemes.

Inspired by developments in aerodynamic boundary-layer theory, an anticipatory, quasi-simultaneous coupling scheme has been developed which intends to circumvent most of the iterative coupling action. Application to two maritime applications, a free-fall life boat and a moored TLP, shows the anticipatory scheme to be robust and rather insensitive to the added-mass ratio.

Future work will focus on more general applications such as interaction of multiple, possibly interconnected, rigid bodies (e.g. the RUG Ocean Grazer [24]).

6 ACKNOWLEDGMENTS

This work is part of the research programme Maritiem 2013 with project number 13267 which is (partly) financed by the Netherlands Organisation for Scientific Research (NWO).

REFERENCES

[1] P. Causin, J.-F. Gerbau, and F. Nobile. Added-mass effect in the design of partitioned algorithms for fluid-structure problems. *Comput. Methods Appl. Mech. Engrg.*, 194:4506–4527, 2005.

[2] Christiane Förster, Wolfgang A. Wall, and Ekkehard Ramm. Artificial added mass instabilities in sequential staggered coupling of nonlinear structures and incompressible viscous flows. *Comput. Meth. Appl. Mech. Engrg.*, 196(7):1278–1293, 2007.

[3] K.C. Park and Carlos A. Felippa. Partitioned analysis of coupled systems. In *Computational Methods for Transient Analysis*, chapter 3, pages 157–219. Elsevier Science

Publishers, Amsterdam, 1983.

[4] Ted Belytschko and Thomas J.R. Hughes, editors. *Computational methods for transient analysis*, volume 1 of *Computational Methods in Mechanics*. Elsevier Science Publishers, Amsterdam, 1983.

[5] K.M.T. Kleefsman, G. Fekken, A.E.P. Veldman, B. Iwanowski, and B. Buchner. A Volume-of-Fluid based simulation method for wave impact problems. *J. Comput. Phys.*, 206:363–393, 2005.

[6] S.M. Hosseini Zahrae, A.E.P. Veldman, P.R. Wellens, I. Akkerman, and R.H.M Huijsmans. The role of a structural mode shape-based interaction law to suppress added-mass instabilities in partitioned strongly-coupled elastic structure-fluid systems. In *Proceedings 36th International Conference on Ocean, Offshore and Arctic Engineering*, Trondheim (Norway), June 25–30, 2017. paper OMAE2017-62075.

[7] R. Verstappen. When does eddy viscosity damp subfilter scales sufficiently? *J. Sci. Comput.*, 49(1):94–110, 2011.

[8] H.J.L. van der Heiden, A.E.P. Veldman, R. Luppes, P. van der Plas, J. Helder, and T. Bunnik. Turbulence modeling for free-surface flow simulations in offshore applications. In *Proceedings 34th International Conference on Ocean, Offshore and Arctic Engineering OMAE2015*, St. John's (Canada), 31 May–5 June, 2015. paper OMAE2015-41078.

[9] A.E.P. Veldman, R. Luppes, P. van der Plas, H.J.L. van der Heiden, J. Helder, and T. Bunnik. Turbulence modeling for locally-refined free-surface flow simulations in offshore applications. In *Proceedings Int Symp Offshore and Polar Eng ISOPE2015*, Kona (Hawaii, USA), 23-27 June, 2015. paper ISOPE2015-TPC-0282.

[10] W. Rozema. *Low-dissipation methods and models for the simulation of turbulent subsonic flow*. PhD thesis, University of Groningen, 2015.

[11] W. Rozema, H.J. Bae, P. Moin, and R. Verstappen. Minimum-dissipation models for large-eddy simulation. *Phys. Fluids*, 27:085107, 2015.

[12] Mahdi Abkar, Hyun J. Bae, and Parviz Moin. Minimum-dissipation scalar transport model for large-eddy simulation of turbulent flows. *Physical Review Fluids*, 1(4):041701, 2016.

[13] M.H. Silvis, F.X. Trias, M. Abkar, H.J. Bae, A. Lozano-Durán, and R.W.C.P. Verstappen. Exploring nonlinear subgrid-scale models and new characteristic length scales for large-eddy simulation. *Proceedings of the CTR Summer Program 2016*. Center for Turbulence Research, Stanford University, pp. 265–274.

[14] R.W.C.P. Verstappen and A.E.P. Veldman. Symmetry-preserving discretization of turbulent flow. *J. Comput. Phys.*, 187:343–368, 2003.

[15] C.W. Hirt and B.D. Nichols. Volume of fluid (VOF) method for the dynamics of free boundaries. *J. Comput. Phys.*, 39:201–25, 1981.

[16] B. Düz. *Wave generation, propagation and absorption in CFD simulations of free surface flows*. PhD thesis, Technical University Delft, 2015.

[17] A.E.P. Veldman. New, quasi-simultaneous method to calculate interacting boundary layers. *AIAA J.*, 19:79–85, 1981.

[18] A.E.P. Veldman. Matched asymptotic expansions and the numerical treatment of viscous-inviscid interaction. *J. Eng. Math.*, 39:189–206, 2001.

[19] A.E.P. Veldman. A simple interaction law for viscous-inviscid interaction. *J. Eng. Math.*, 65:367–383, 2009.

[20] Arthur E.P. Veldman. 'Missing' boundary conditions? Discretize first, substitute next, and combine later. *SIAM J. Sci. Stat. Comput.*, 11(1):82–91, 1990.

[21] P. van der Plas, A.E.P. Veldman, H.J.L. van der Heiden, and R. Luppes. Adaptive grid refinement for free-surface flow simulations in offshore applications. In *Proceedings 34th International Conference on Ocean, Offshore and Arctic Engineering OMAE2015*, St. John's (Canada), 31 May–5 June, 2015. paper OMAE2015-42029.

[22] P. van der Plas. *Local grid refinement for free-surface flow simulations*. PhD thesis, University of Groningen, 2017.

[23] E.F.F. Botta and M.H.M. Ellenbroek. A modified SOR method for the Poisson equation in unsteady free-surface flow calculations. *J. Comput. Phys.*, 60:119–134, 1985.

[24] W.A. Prins, et al. Ocean grazer project. University of Groningen. URL: www.oceangrazer.com.